The Brazilian Journal of
INFECTIOUS DISEASES

www.elsevier.com/locate/bjid

Original Article

Influence of microbiome species in hard-to-heal wounds on disease severity and treatment duration

Dagmar Chudobova[a,b], *Kristyna Cihalova*[a,b], *Roman Guran*[a,b], *Simona Dostalova*[a,b], *Kristyna Smerkova*[a,b], *Radek Vesely*[c], *Jaromir Gumulec*[a,d], *Michal Masarik*[a,d], *Zbynek Heger*[a,b], *Vojtech Adam*[a,b], *Rene Kizek*[a,b,*]

[a] *Department of Chemistry and Biochemistry, Mendel University in Brno, Zemedelska, Czech Republic*
[b] *Central European Institute of Technology, Brno University of Technology, Technicka, Czech Republic*
[c] *Department of Traumatology at the Medical Faculty, Masaryk University and Trauma Hospital of Brno, Ponavka, Czech Republic*
[d] *Department of Pathological Physiology, Faculty of Medicine, Masaryk University, Kamenice, Czech Republic*

ARTICLE INFO

Article history:
Received 9 January 2015
Accepted 8 August 2015
Available online 27 October 2015

Keywords:
Bacterial strains
MALDI-TOF
Sequencing
Superficial wounds

ABSTRACT

Background: Infections, mostly those associated with colonization of wound by different pathogenic microorganisms, are one of the most serious health complications during a medical treatment. Therefore, this study is focused on the isolation, characterization, and identification of microorganisms prevalent in superficial wounds of patients ($n = 50$) presenting with bacterial infection.

Methods: After successful cultivation, bacteria were processed and analyzed. Initially the identification of the strains was performed through matrix-assisted laser desorption/ionization time-of-flight mass spectrometry based on comparison of protein profiles (2–30 kDa) with database. Subsequently, bacterial strains from infected wounds were identified by both matrix-assisted laser desorption/ionization time-of-flight mass spectrometry and sequencing of 16S rRNA gene 108.

Results: The most prevalent species was *Staphylococcus aureus* (70%), and out of those 11% turned out to be methicillin-resistant (*mecA* positive). Identified strains were compared with patients' diagnoses using the method of artificial neuronal network to assess the association between severity of infection and wound microbiome species composition. Artificial neuronal network was subsequently used to predict patients' prognosis ($n = 9$) with 85% success.

* *Corresponding author.*
E-mail address: kizek@sci.muni.cz (R. Kizek).
http://dx.doi.org/10.1016/j.bjid.2015.08.013

Conclusions: In all of 50 patients tested bacterial infections were identified. Based on the proposed artificial neuronal network we were able to predict the severity of the infection and length of the treatment.

Introduction

Skin has an important role in preventing the entry of undesirable substances, organisms, and bacteria into the bloodstream.[1,2] Loss of skin integrity leads to different types of wounds which have the humidity, warmth, and a nurturing environment ideal for colonization and proliferation of undesirable bacterial strains, changing the naturally occurring microbiome. Colonized sites are usually polymicrobial, *i.e.* contain more than one bacterium with pathogenic potential.[3] Wound infections are marked by disturbed host–bacteria equilibrium in a traumatized tissue environment favoring the pathogenic bacteria. A wound infection not only has the possibility to elicit a systemic response (sepsis), but is also able to inhibit the multiple processes involved in the orchestrated progression of normal wound healing.[4]

The concept of microbiome was first suggested in 2001 by Lederberg and McCray and was described as an ecological cohort of commensal, symbiotic, and pathogenic microorganisms sharing a body space.[5] Previously, it was estimated that as much as 20 to 60% of human-associated microbiome is hard-to-identify, which has likely resulted in an underestimation of microbiome diversity.[6] One of the most frequent microorganisms in infected wound is *Staphylococcus aureus*.[7–10] According to numerous studies,[11–13] another common organism in infected wounds is *Pseudomonas aeruginosa* with up to 10% occurrence, causing nosocomial infections together with *S. aureus* and other bacteria. In addition, the *Enterobacteriaceae* family is most often identified in connection with immunocompromised patients or those who have undergone abdominal surgery.[1]

Bacterial infections, increasingly occurring in medical facilities, can seriously complicate the outcome of treated patients.[14,15] This is particularly connected with rising resistance of bacterial strains toward antibiotics or metals,[16,17] thus significantly hindering treatment success. Although being highly debated the mechanism of resistance development has not been satisfactorily elucidated.[18–21]

The elevated occurrence of resistant bacterial strains is strictly linked with increased utilization of invasive surgical techniques, which are often performed in elderly, immunocompromised patients. Simultaneously, with the use of antibiotics, bacterial resistance can evolve in surgical sites, leading to bacteremia and sepsis, and thus significantly prolonging the healing phase of a patient. Although bacterial resistance presents a problem in healthcare facilities, there still exist few possibilities to eliminate the most frequent resistant strains that cause hospital-acquired infection – methicillin-resistant *S. aureus* (MRSA),[22,23] *e.g.* highly potent glycopeptide vancomycin.[24] However, for a correct choice of antibiotics one needs to accurately identify the microbiome composition of infected wounds. Knowledge of the bacterial ecology of wounds may thus lead to increase treatment success, coupled with curbing bacterial resistance as a result of inadequate utilization of antibiotics.[25–28]

Accordingly, this work is focused on identification of the microbiome associated with serious infections in hard-to-heal wounds with the aim to propose a prediction model, comprising both the microbiome composition and patients´health conditions.

Materials and methods

Chemicals, preparation of deionized water and pH measurement

Chemicals used in this study were acquired from Sigma-Aldrich (St. Louis, MO, USA) in ACS purity unless noted otherwise. Deionized water was prepared using reverse osmosis equipment Aqual 25 (Aqual s.r.o., Brno, Czech Republic) and further purified using Milli-Q Direct QUV equipped with the UV lamp, with 18 MΩ resistance. pH was measured using the pH meter WTW inoLab (Weilheim, Germany).

Preparation of hospital samples and their cultivation

Cohort of patients with bacterial infections

For evaluation, patients with superficial or deep wounds were selected according to infection severity. Detailed information concerning the patients is documented in S1. A total of 50 patients aged 19 through 93 years were enrolled into the clinical study, and 13 patients were 70–79 years old; 23 patients superficial wounds and 27 deep wounds. For all patients, the treatment duration was determined by the traumatologist based severity and extent of infection, associated diseases potentially interfering with treatment outcome and healing of wounds, and other factors such as patient age, concomitant medications, and previous medical history. For confirmation of the functionality of the neural network 9 blank samples from 9 patients identified by MALDI-TOF MS were used. Enrollment of patients into the clinical study was approved by the Ethics Committee of Trauma hospital in Brno.

Collection of wound swabs from patients with bacterial infections

The smears, collected from infected wounds with the agreement of patients, were sampled by rolling motion at the wound using a sterile swab sampler. All patients were divided into two subgroups, on the grounds of infection severity: deep and superficial wound. A detailed description of comorbidities and duration of treatment was obtained. Patients were classified

according to the Classification of surgical wounds – SSI (surgical site infections).[29–31] Infected wounds were sampled by using disposable tampon swabs maximizing collection of representative microflora. Tampons were subsequently stored in transport medium (inorganic salts, sodium thioglycolate, 1% agar, activated charcoal). The important part of our workflow process comprised sampling in duplicates with further transport in both aerobic and anaerobic conditions to preserve bacterial viability.

Cultivation of clinical specimens

Four types of selective nutrient media (blood agar enriched by 10% NaCl, Endo agar, blood agar without any other component, and blood agar with amikacin) we employed for further microbiological selection. Petri dishes, containing the above mentioned media were subsequently incubated according to conventional protocols, as described elsewhere,[32–35] to maintain suitable conditions for growth of all types of bacteria. These Petri dishes were incubated for 24–48 h at 37 °C supplemented by TGY medium (1 g L^{-1} glucose, 5 g L^{-1} tryptone, 2.5 g L^{-1} yeast extract). Subsequently, individual colonies were collected from each Petri dish and stored in 1 μL of enriched media. These samples were processed as described in the *DNA sequencing* section and utilized for both – MALDI-TOF MS identification and PCR with subsequent sequencing.

MALDI-TOF MS identification of bacteria

The following extraction protocol was based on MALDI Biotyper™ 3.0 User Manual Revision 2, also used in a previous report.[36] 500 μL of bacterial culture, cultivated overnight, was centrifuged at 14,000 × *g* for 2 min. The supernatant was discarded and the pellet was re-suspended in 300 μL of deionized water besides adding 900 μL of ethanol. After centrifugation at 14,000 × *g* for 2 min, the supernatant was discarded and the obtained pellet was air-dried. The pellet was then dissolved in 25 μL of 70% formic acid (*v*/*v*) and 25 μL of acetonitrile and mixed. The samples were centrifuged at 14,000 × *g* for 2 min and 1 μL of the clear supernatant was spotted in duplicate onto the MALDI target and air-dried at room temperature. Then, each spot was overlaid with 1 μL of α-cyano-4-hydroxycinnamic acid (HCCA) matrix solution (20 mg mL^{-1}) in organic solvent (50% acetonitrile and 2.5% trifluoroacetic acid, both *v*/*v*) and air-dried completely prior to MALDI-TOF MS measurement on UltrafleXtreme MS (Bruker Daltonik GmbH, Bremen, Germany). As matrix solution 2,5-dihydroxybenzoic acid (DHB) was also used in the same concentration and solvent as HCCA. Spectral data were taken in the *m*/*z* range of 2000–30,000 Da, resulted from the accumulation of 240 laser shots targeted to different regions of the same sample spot. These data were analyzed with the Flex Analysis software (Version 3.4). Final preparation of dendrograms was carried out in the MALDI BioTyper™ 3.1 (Bruker Daltonik GmbH, Bremen, Germany).

DNA sequencing

Bacterial cells were centrifuged at 4450 × *g* and 20 °C for 10 min. The pellet was resuspended in 400 μL of lysis buffer (6 M guanidium hydrochloride, 0.1 M sodium acetate) and cells were lysed for 1 hour at 20 °C and 600 rpm on Multi RS-60 (Biosan, Riga, Latvia). Genomic DNA was isolated from lysed bacterial cultures *via* MagNA Pure Compact (Roche, Mannheim, Germany), using Nucleic Acid Isolation Kit I, protocol DNA_Bacteria.

16S rRNA gene was amplified using *Taq* PCR Mix (New England Biolabs, Ipswich, MA, USA) and MasterCycler realplex[4] epgradient S (Eppendorf, Hamburg, Germany). 100 μL of reaction mixture consisted of: 1× Standard *Taq* Reaction Buffer, 1.6 U of *Taq* DNA polymerase, 200 μM Deoxynucleotide Solution Mix, 0.5 μM primers and 5 μL of isolated genomic DNA. The forward primer E9F 5′-GAGTTTGATCCTGGCTCAG-3′ and reverse primer U1510R 5′-GGTTACCTTGTTACGACTT-3′ were synthesized by Sigma–Aldrich (St. Louis, MO, USA). The reaction profile was as follows: initial denaturation at 94 °C for 4 min; 30 cycles of denaturation at 94 °C for 30 s, annealing at 52 °C for 30 s and elongation at 72 °C for 105 s; with terminal elongation at 72 °C for 10 min. Amplified fragments were purified using MinElute PCR Purification Kit (Qiagen, Hilden, Germany).

For sequencing reaction the DTCS Quick Start Kit (Beckman Coulter, Pasadena, CA, USA) was used. To 20 μL sequencing reaction mixture, 98 ng of purified fragment, 0.75 μL of 10 μM forward primer, 4 μL of DTCS Quick Start Master Mix and 1 μL of Sequencing Buffer were added. The conditions of 30 cycle-reactions were as follows: 96 °C for 20 s; 50 °C for 20 s and 60 °C for 4 min. The purification of sequencing product was carried out using CleanSEQ kit (Beckman Coulter). Purified samples in Sample Loading Solution were transferred to the plate and DNA sequencing was performed using Genetic Analysis System CEQ 8000 (Beckman Coulter). After denaturation at 90 °C for 2 min, a fluorescence-marked DNA fragments were separated in 33 cm long capillary with 75 μm i.d. (Beckman Coulter) filled with linear polyacrylamide denaturing gel. The separation was run at capillary temperature of 50 °C and voltage of 4.0 kV for 85 min. Sequences were identified by comparison with NCBI database.

Amplification of S. aureus genes mecA and fnbA

Isolation of genomic DNA was performed using the same method as described in section *DNA sequencing*. The *mecA* and *fnbA* genes were amplified using polymerase chain reaction (PCR) as previously reported.[37] The primers were synthesized by Sigma-Aldrich and the sequences of forward and reverse primers for *mecA* gene were 5′-CCCAATTTGTCTGCCAGTTT-3′, and 5′-TGGCAATATTAACGCACCTC-3′ and for *fnbA* gene were 5′-GATACAAACCCAGGTGGTGG-3′, and 5′-TGTGCTTGACCATGCTCTTC-3′. The volume of PCR reaction mixture was 100 μL containing 1× *Taq* reaction buffer, 0.2 mM dNTP, 1.6 U of *Taq* DNA polymerase (New England Biolabs) and 0.5 mM of each primer. The reaction profile was as follows: initial denaturation at 94 °C for 4 min, 30 cycles of denaturation at 94 °C for 30 s, annealing at 53 °C for 30 s and extension at 72 °C for 1 min with a final extension of 7 min. The amplification generated a 223 bp for *mecA* and 191 bp for *fnbA*.

Agarose gel (2% (*v*/*v*), high melt, Mercury, San Diego, CA, USA) was prepared with 1× TAE buffer (40 mM Tris, 20 mM acetic acid and 1 mM ethylenediaminetetraacetic acid) and ethidium bromide (5 μL per 100 mL of the gel) as described

elsewhere.[38] 100 bp DNA ladder (New England Biolabs) within the size range from 100 to 1517 bp was used to monitor the size of the analyzed fragment. The electrophoresis (Bio-Rad, Hercules, CA, USA) was run at 60 V and 6 °C for 160 min. The bands were visualized by UV transilluminator at 312 nm (Vilber-Lourmant, Marne-la-Vallée, France).

Statistical processing of obtained results

Automated neuronal network was used as a predictive model. Classification analysis automated neuronal network was used for the estimation of categorical data. The dataset was randomly divided as follows: 80% for learning, 10% for testing, and 10% for validation. Following network types were tested using automated network search: multilayer perceptron network (MLP), and radial basis function (RBF). Number of hidden units to search was determined as follows: 8–24 and 8–11 for MLP and RBF, respectively. Total 1000 networks were trained, and activation functions were searched for identity, logistic, tanh, exponential. Weight decay of 0.0001–0.001 was used for hidden layer and output layer. Weight of input variables for learning was used based on MALDI-TOF classification score. Unless noted otherwise, *p*-value less than 0.05 was considered significant. Software Statistica 12 (StatSoft, CA, USA) was used for analysis.

Results and discussion

We decided to employ a variety of cultivation approaches (in presence of O_2, CO_2 or in microaerophilic conditions) to reveal the presence of real microbiota associated with superficial infections.

MALDI-TOF MS was explored as an accurate and rapid identification tool, using the protein mass patterns, which are compared with patterns from a commercial Bruker Daltonics database (BDAL) of MALDI Biotyper™ software.[39] Due to a powerful software support, the method can be used for identification within few minutes, which is one of the advantages.[36] Moreover, sequencing of amplified 16S rRNA gene[40] was employed for identification independent of protein patterns. Finally, an artificial neural network (ANN) was developed as a predictive model for evaluation of infection severity and using developed ANN we attempted to find the relationship between disease severity and the microorganisms identified in clinical specimens.

Identification of bacterial strains by MALDI-TOF MS and Sanger sequencing

For the identification of bacterial entities we employed complementary methods for independent evaluation of different biomolecules – proteins and DNA.[36,41,42] Sanger sequencing was utilized as a confirmation method, based on sequencing of 16S rRNA gene. This gene contains hypervariable regions, providing species-specific sequences, hence it can provide enough information for a confident discrimination, and thus became popular in medical microbiology to classify bacteria.[43,44]

When compared to sequencing, MALDI-TOF MS offers much shorter analysis time. By using this technique, wound microbiome could be discriminated within one hour of incubation, and thus this will likely become the method of choice for future microbiome identification. Nevertheless, the classification is based on a still developing database[34]; hence MALDI-TOF MS identification of non-databased bacteria has still to be connected with other confirmation methods. From this reason we firstly employed MALDI-TOF MS with a condition: If score <2.00 = 16S rRNA sequencing.

As shown in S2, 108 bacterial strains were identified[37] of them had to be confirmed by sequencing and confirmed strains were immediately databased to increase future classification success. Strains of *S. aureus* were the most often identified ($n = 35$). Thus, methicillin-resistant *S. aureus* (MRSA) is highly associated with severe infections in post-surgical wounds[45]; we further analyzed the *mecA* gene, encoding a modified penicillin binding protein (PBP) known as PBP2a, with decreased affinity toward β-lactams.[46] The *mecA* positivity was determined in four isolates. Since 67% of patients had deep wound infections and were treated for more than 8 weeks after admission to infectious Department of Trauma Hospital of Brno, presence of *mecA* was shown to be a crucial microbiological factor, affecting patients prognosis. Further, we determined the presence of *fnbA* gene, responsible for adhesins production. Adhesion to human extracellular matrix components and serum proteins is an important facet in the interaction between bacteria and its host cells.[47] Lim and coworkers identified the presence of *fnbA* in 96% of all isolated MRSA strains.[35] In our case, *fnbA* presence was confirmed in all MRSA isolates and in 89% of methicillin-sensitive *S. aureus* isolates. Similarly to *mecA*, *fnbA* was found to be associated with infection severity. In patients with negative *fnbA* and *mecA* the treatment duration was less than four weeks in 75% of cases, despite the fact that patients had deep wound infections. This finding suggests that the severity of staphylococcal infections does not depend solely on antimicrobial resistance, but also on adhesins expression, which enhance the interaction with the target host cells.

Distribution of identified strains within various cohorts of patients

According to duration of treatment, the patients were divided into specific subgroups, where each sector represents one bacterial strain.

The subdivision of patients was based on surgical wounds classification SSI. As shown, patients were divided into two groups - deep and superficial wounds and the associated bacterial strains are depicted in Fig. 1A and B.

As it is obvious from Fig. 1A, in the more serious infections (deep) *S. aureus* was the main bacterium of microbiome composition (28% of identified strains), followed by *Enterococcus faecalis* (15%), and *Escherichia coli* (11%). On the other hand, *E. coli* was not so often identified in surficial wounds (5% – Fig. 1B). Taken together, the microbiome composition in both groups exhibits substantial differences, and thus it can be hypothesized that presence of minority representatives as *Hafnia alvei*, *Proteus vulgaris*, *Staphylococcus lugdunensis*, or

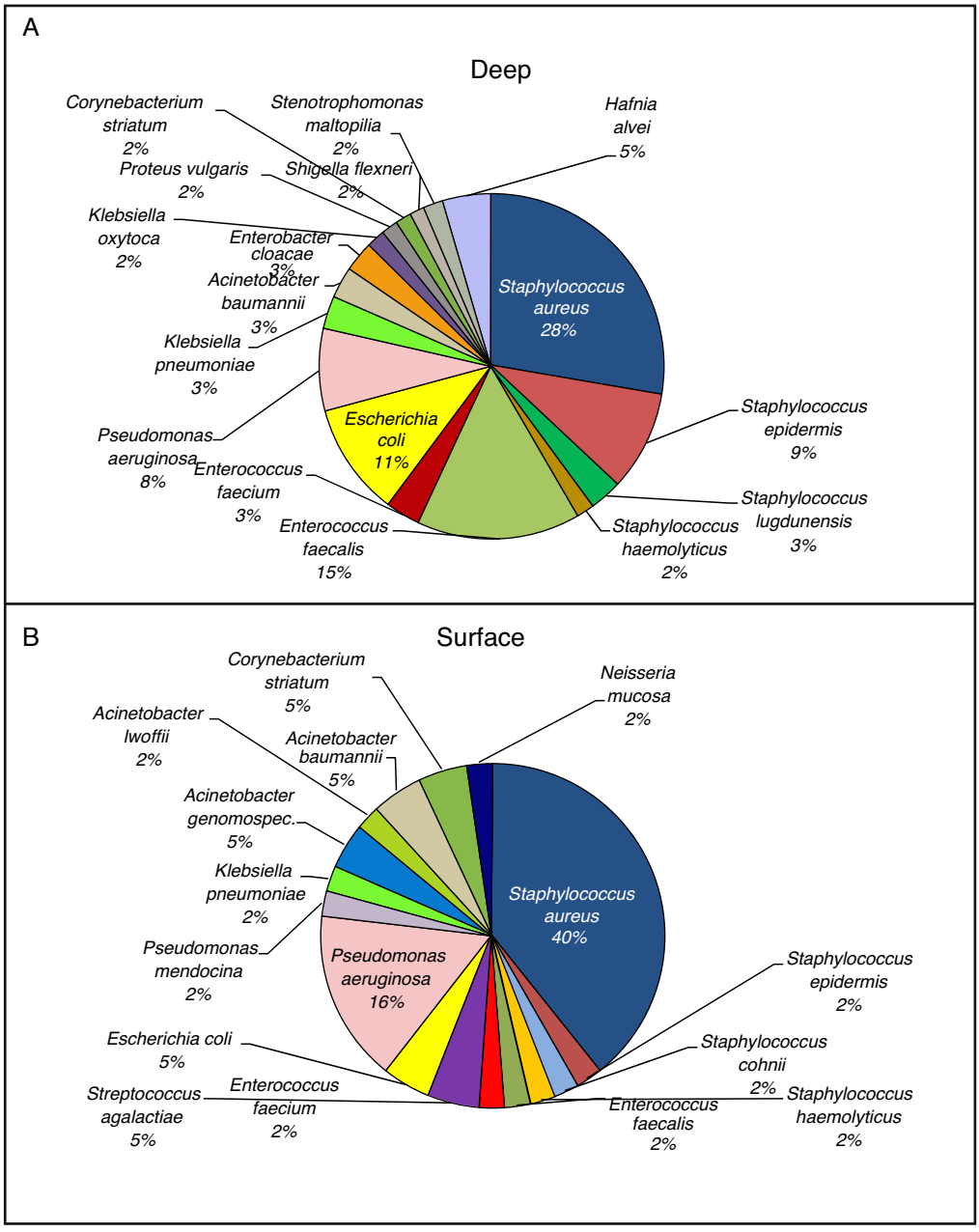

Fig. 1 – Representation of microorganism species present in patients' wounds. Patients were grouped based on infection severity. The graphs show bacterial cultures grown on different selective nutrient media. (A) Infection severity – deep wounds and (B) infection severity – superficial wounds.

Enterobacter cloacae in the wound can significantly influence the infection severity. It can be also stated that increasing duration of treatment leads to increased number of identified *Enterobacteriaceae* and opportunistic pathogens (*Pseudomonas*, *Enterococcus*).

Phylogenetic analysis of protein alterations

As was shown by Rettinger and colleagues,[48] MALDI-TOF mass spectra-based phylogenetic analysis is considered equivalent to 16S rRNA gene sequencing. Therefore, we employed MALDI Biotyper™ for preparation of dendrograms for our groups, divided by treatment duration (Fig. 2). Dendrograms showed similarity of same bacterial strains (low distance level), but in some cases larger differences were found – usually among bacterial strains from different patients. These differences were caused probably by modifications of bacterial proteins. Karger et al. found methylation as a cause of higher distance level in dendrogram between *Burkholderia pseudomallei* and other types of *B. pseudomallei*.[49] Thus it can be concluded that not only changes in microbiome representatives affect treatment duration and success, but also small changes in protein post-translation modifications can be highly important for patients' recovery.

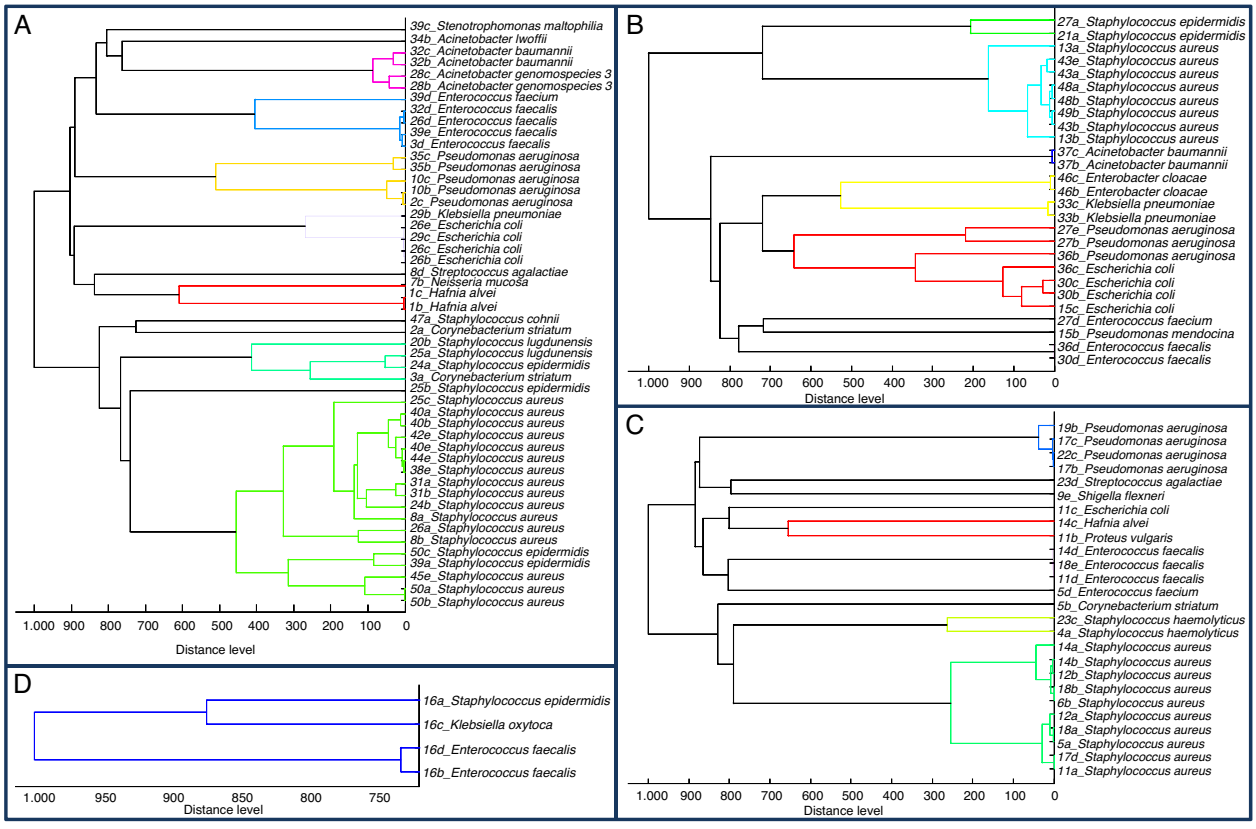

Fig. 2 – Dendrograms from protein mass profiles of microorganisms in different groups based on treatment duration. Created in MALDI Biotyper™. (A) Treatment duration less than four weeks. (B) Treatment duration 4–7 weeks. (C) Treatment duration eight and more weeks. (D) Exitus.

Artificial neural network

Two neuronal networks were created: (1) for the prediction of time-to-heal, and (2) for the prediction of infection severity. The following input parameters were used for the construction of networks: from 2000 networks five were retained and one was used for further final custom neuronal network. The settings of the network created using automated algorithm and used for the custom final learning were Multilayer perceptron 89-13-3 (input-hidden-output neurons), Broyden–Fletcher–Goldfarb–Shanno (BFGS) training algorithm, sum of squares error function, identity function for hidden layer, and then for output layer. The design of the network is displayed in Fig. 3A. With stopping conditions enabled (Fig. 3B), a final network was created in the 17th training cycle with performances of 91.4%, 85.7%, and 71.4% for training, testing, and validation (accuracy in prediction up to 85% – Fig. 3C), respectively.

Consequently, a second neuronal network for the prediction of infection severity was created using an automated algorithm. The best-performing network was trained under following settings: multilayer perceptron 89-19-2 (input-hidden-output neurons) (Fig. 3D) BFGS training algorithm, cross entropy error function, and exponential and softmax activation function for hidden and output layer. The training process is depicted in Fig. 3E (accuracy in prediction up to 85% – Fig. 3F).

The performances of the network were 100.0%, 85.7%, and 85.7% for training, testing, and validation (Table 1), respectively. The accuracy for individual cases is displayed in Table 2.

Sensitivity analysis of input variables for both networks was carried out. For the prediction of infection severity,

Table 1 – Characterization of neuronal network performance for the prediction of patient outcome. Performance displayed in % for training, testing, and validation samples. The number of training cycle for custom network training is displayed in training algorithm column. BFGS, Broyden–Fletcher–Goldfarb–Shanno training algorithm; SOS, sum of squares.

Prediction target	Net. name	Performance			Training algorithm	Error function	Activation	
		Training	Testing	Validation				Train
Infection severity	MLP 89-19-2	100.00	85.71	85.71	BFGS 24	Infection severity	MLP 89-19-2	100.00
Time-to-heal	MLP 89-13-3	91.43	85.71	71.43	BFGS 17	Time-to-heal	MLP 89-13-3	91.43

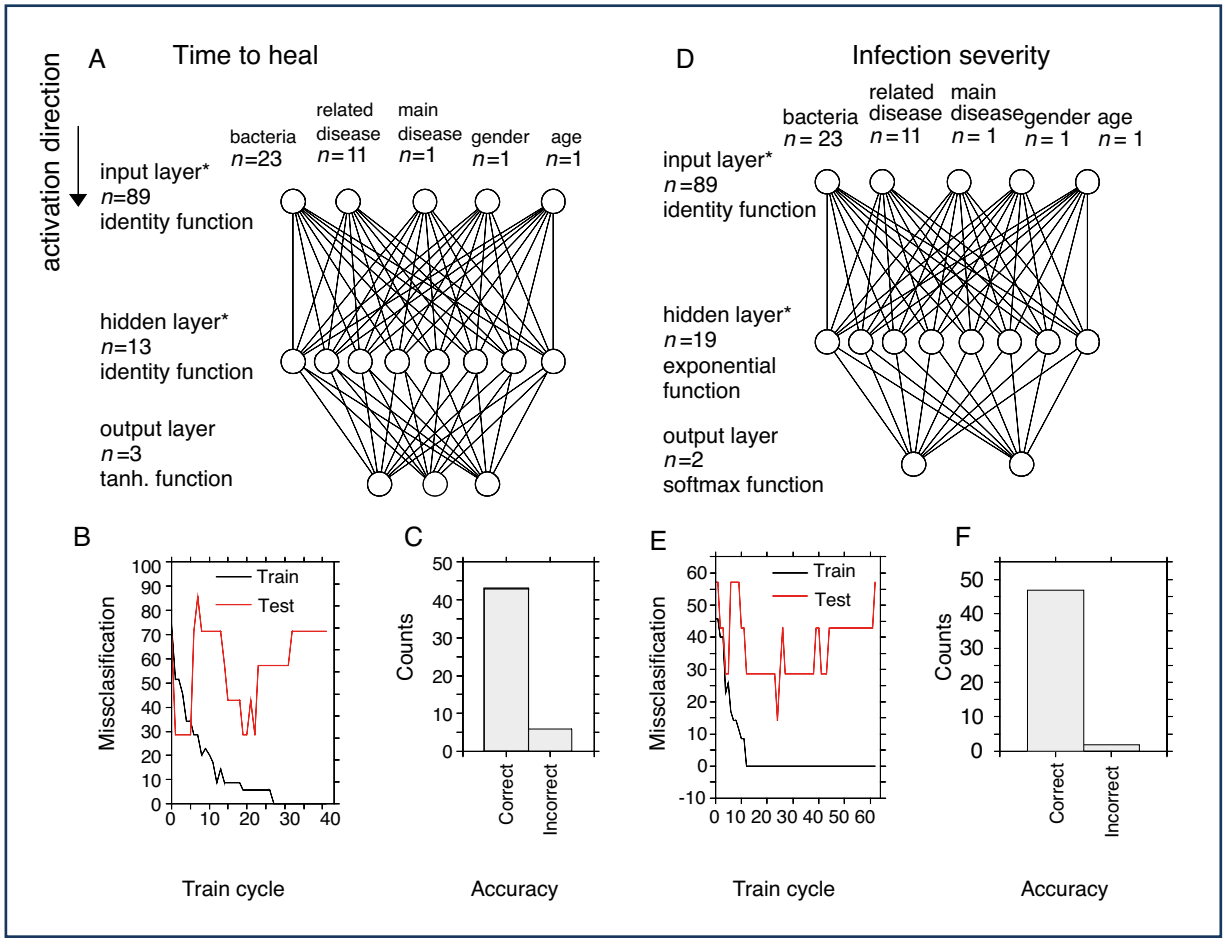

Fig. 3 – Design and performance of the neuronal networks. (A) Design of classification network for the prediction of time-to-heal. The number of neurons/inputs is indicated by *n*. *Note the number of input and hidden neurons is not displayed exactly. (B) Training process of the classification network with stopping conditions activated. (C) Accuracy of the final network for classification of time-to-heal. (D) Design of classification network for the prediction of infection severity. (E) Training process for creation of this network with stopping criteria activated. (F) Accuracy of the network for the prediction of infection severity.

Table 2 – Performance of the network: verification of the test and validation cohort. Analysis for both networks for prediction of infection severity and time-to-heal. Test cohort was employed for stopping conditions. Validation sample was used to test final network. "target" indicates input data, network output reflects calculated result from the neuronal network. id, identification of patient; w, week.

Sample	ID	Case weights	Infection severity				Time-to-heal			
			Target	Network output	Accuracy	Conf. level	Target	Network output	Accuracy	Conf. level
Test	2	1.71	Superficial	Superficial	Correct	1.00	<4 w	<4 w	Correct	0.40
	6	1.81	Deep	Deep	Correct	1.00	>8 w	<4 w	Incorrect	0.47
	8	1.65	Superficial	Superficial	Correct	1.00	<4 w	<4 w	Correct	0.36
	22	2.00	Superficial	Superficial	Correct	1.00	>8 w	>8 w	Correct	0.41
	38	2.06	Deep	Superficial	Incorrect	1.00	<4 w	<4 w	Correct	0.49
	39	2.01	Deep	Deep	Correct	1.00	<4 w	<4 w	Correct	0.56
	40	2.12	Superficial	Superficial	Correct	1.00	<4 w	<4 w	Correct	0.43
Validation	7	1.68	Superficial	Deep	Incorrect	1.00	<4 w	<4 w	Correct	0.40
	23	1.62	Superficial	Superficial	Correct	1.00	>8 w	>8 w	Correct	0.49
	27	2.23	Deep	Deep	Correct	0.87	4–7 w	<4 w	Incorrect	0.58
	28	2.11	Superficial	Superficial	Correct	1.00	<4 w	<4 w	Correct	0.47
	36	2.27	Deep	Deep	Correct	1.00	4–7 w	4–7 w	Correct	0.63
	45	1.88	Deep	Deep	Correct	1.00	<4 w	<4 w	Correct	0.43
	49	2.25	Deep	Deep	Correct	1.00	4–7 w	<4 w	Incorrect	0.56

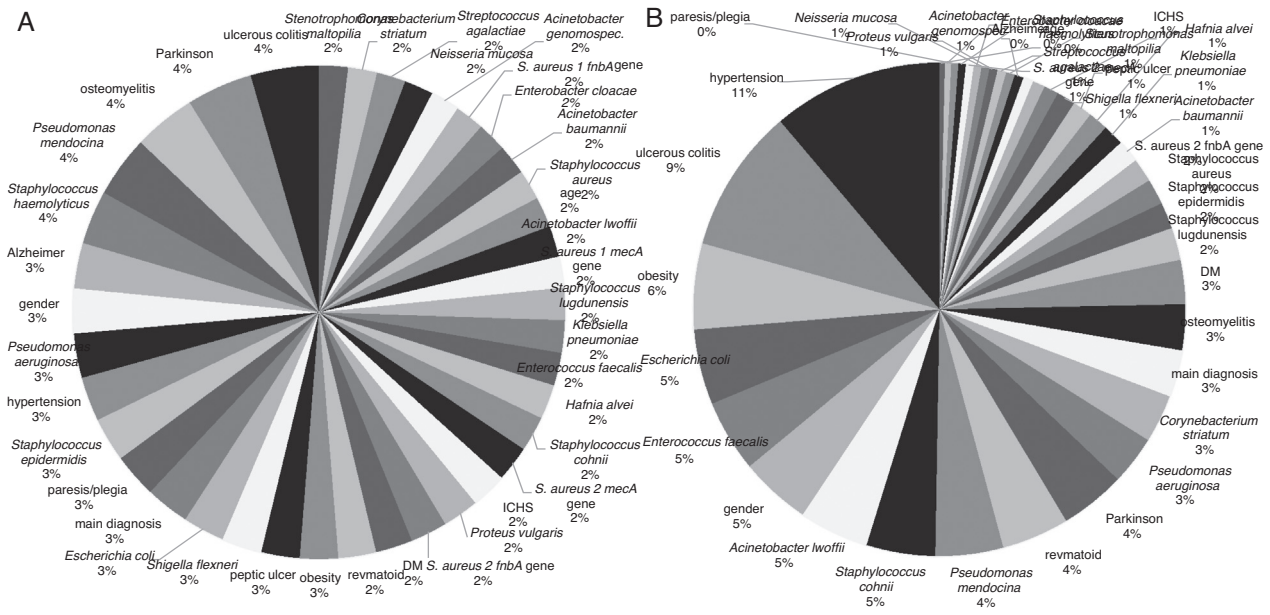

Fig. 4 – Sensitivity analysis of all factors for prediction of time-to-heal and infection severity. Sensitivity of individual factors depicted as a percentage of total sensitivity. (A) Sensitivity of individual factors for the prediction of time-to-heal. (B) Sensitivity of individual factors for the prediction of infection severity.

the mean sensitivity level was 4.66, ranging from 0.63 to 20.1, and a total sensitivity = 179.9 (Fig. 4) The highest level of sensitivity (thus highest impact on prediction of a network) was observed for hypertension (20.15), ulcerative colitis (17.06), obesity (10.13), *E. coli* (8.87), *E. faecalis* (8.50), and other factors. The factors with sensitivity <1 were *P. vulgaris*, *Neisseria mucosa*, *E. cloacae*, *S. aureus* 2 *mecA* genes, *Staphylococcus haemolyticus*, paresis/plegia, Alzheimer's disease, age.

For the prediction of time-to-heal, the sensitivity was distinctly more homogeneous for the input factors with mean sensitivity = 1.35, (0.99–2.35), total sensitivity = 52.49. The factors with higher sensitivity included ulcerative colitis (2.35), Parkinson's disease (2.27), osteomyelitis (2.15), *Pseudomonas mendocina* (2.11), *S. haemolyticus* (1.84) and others (Fig. 4). The factors with sensitivity <1 include *Streptococcus agalactiae*, *Corynebacterium striatum*, and *Stenotrophomonas maltopilia*.

Conflicts of interest

The authors declare no conflicts of interest.

AcknowledgementS

The study was financially supported by CEITEC CZ.1.05/1.1.00/02.0068. The authors wish also to express their special thanks to Radek Chmela for perfect technical assistance.

Appendix A. Supplementary data

Supplementary data associated with this article can be found, in the online version, at http://dx.doi.org/10.1016/j.bjid.2015.08.013.

REFERENCES

1. Mama M, Abdissa A, Sewunet T. Antimicrobial susceptibility pattern of bacterial isolates from wound infection and their sensitivity to alternative topical agents at Jimma University Specialized Hospital, South-West Ethiopia. Ann Clin Microbiol Antimicrob. 2014;13:1–10.
2. Ndip RN, Malange Takang AE, Echakachi CM, et al. In-vitro antimicrobial activity of selected honeys on clinical isolates of *Helicobacter pylori*. Afr Health Sci. 2007;7:228–32.
3. Dai T, Huang YY, Sharma SK, Hashmi JT, Kurup DB, Hamblin MR. Topical antimicrobials for burn wound infections. Recent Patents Anti-infect Drug Discov. 2010;5:124–51.
4. Dai TH, Tanaka M, Huang YY, Hamblin MR. Chitosan preparations for wounds and burns: antimicrobial and wound-healing effects. Expert Rev Anti-Infect Ther. 2011;9:857–79.
5. Lederberg J, McCray AT. 'Ome sweet' omics – a genealogical treasury of words. Scientist. 2001;15:8–9.
6. Bik EM, Eckburg PB, Gill SR, et al. Molecular analysis of the bacterial microbiota in the human stomach. Proc Natl Acad Sci U S A. 2006;103:732–7.
7. Polaczek-Kornecka B, Dziadur-Goldsztaj Z, Turowski G. Methicillin-oxacillin resistant strains of *Staphylococcus aureus* (MORSA) in infected burn wounds. Mater Med Polona Polish J Med Pharm. 1991;23:304–5.
8. Cooper RA, Molan PC, Harding KG. Antibacterial activity of honey against strains of *Staphylococcus aureus* from infected wounds. J R Soc Med. 1999;92:283–5.
9. Simonetti O, Cirioni O, Ghiselli R, et al. RNAIII-inhibiting peptide enhances healing of wounds infected with methicillin-resistant *Staphylococcus aureus*. Antimicrob Agents Chemother. 2008;52:2205–11.
10. Lima AF, Costa LB, da Silva JL, Maiaiv MBS, Ximenes E. Interventions for wound healing among diabetic patients infected with *Staphylococcus aureus*: a systematic review. Sao Paulo Med J. 2011;129:165–70.

11. Ricotti CA Jr, Cazzaniga A, Feiner A, Davis SC, Mertz PM. Epifluorescent microscopic visualization of an in-vitro biofilm formed by a *Pseudomonas aeruginosa* wound isolate and of an in-vivo polymicrobial biofilm obtained from an infected wound. Abst General Meeting Am Soc Microbiol. 2003;103. J-023.
12. Schmoldt S, Ozkaya I, Gotzfried M, Heesemann J, Hogardt M. Pathotyping of *Pseudomonas aeruginosa* isolated from chronically infected wounds. Int J Med Microbiol. 2007;297:114–5.
13. Wildeboer D, Hill KE, Jeganathan F, et al. Specific protease activity indicates the degree of *Pseudomonas aeruginosa* infection in chronic infected wounds. Eur J Clin Microbiol Infect Dis. 2012;31:2183–9.
14. Chudobova D, Cihalova K, Dostalova S, et al. Comparison of the effects of silver phosphate and selenium nanoparticles on *Staphylococcus aureus* growth reveals potential for selenium particles to prevent infection. FEMS Microbiol Lett. 2014;351:195–201.
15. Hoerr V, Zbytnuik L, Leger C, Tam PPC, Kubes P, Vogel HJ. Gram-negative and Gram-positive bacterial infections give rise to a different metabolic response in a mouse model. J Proteome Res. 2012;11:3231–45.
16. Chudobova D, Dostalova S, Blazkova I, et al. Effect of ampicillin, streptomycin, penicillin and tetracycline on metal resistant and non-resistant *Staphylococcus aureus*. Int J Environ Res Public Health. 2014;11:3233–55.
17. Chudobova D, Dostalova S, Ruttkay-Nedecky B, et al. The effect of metal ions on *Staphylococcus aureus* revealed by biochemical and mass spectrometric analyses. Microbiol Res. 2015;170:147–56.
18. Nasim A, Thompson MM, Naylor AR, Bell PRF, London NJM. The impact of MRSA on vascular surgery. Eur J Vasc Endovasc Surg. 2001;22:211–4.
19. Young MH, Upchurch GR, Malani PN. Vascular graft infections. Infect Dis Clin North Am. 2012;26:41–56.
20. Anderson DJ, Sexton DJ, Kanafani ZA, Auten G, Kaye KS. Severe surgical site infection in community hospitals: epidemiology, key procedures, and the changing prevalence of methicillin-resistant *Staphylococcus aureus*. Infect Control Hosp Epidemiol. 2007;28:1047–53.
21. Earnshaw JJ. Methicillin-resistant *Staphylococcus aureus*: vascular surgeons should fight back. Eur J Vasc Endovasc Surg. 2002;24:283–6.
22. Zhang J, Liu HC, Zhu KK, et al. Antiinfective therapy with a small molecule inhibitor of *Staphylococcus aureus* sortase. Proc Natl Acad Sci U S A. 2014;111:13517–22.
23. Solis N, Parker BL, Kwong SM, Robinson G, Firth N, Cordwell SJ. *Staphylococcus aureus* surface proteins involved in adaptation to oxacillin identified using a novel cell shaving approach. J Proteome Res. 2014;13:2954–72.
24. Rolston KVI, Wang WQ, Nesher L, Coyle E, Shelburne S, Prince RA. In vitro activity of telavancin compared with vancomycin and linezolid against Gram-positive organisms isolated from cancer patients. J Antibiot. 2014;67:505–9.
25. Wang DH, Yuan JF, Tao WY. Identification of a novel antibiotic from myxobacterium stigmatella eracta WXNXJ-B and evaluation of its antitumor effects in-vitro. Iran J Pharm Res. 2014;13:171–80.
26. Verma MS, Chen PZ, Jones L, Gu FX. Chemical nose for the visual identification of emerging ocular pathogens using gold nanostars. Biosens Bioelectr. 2014;61:386–90.
27. Strompfova V, Laukova A. Isolation and characterization of faecal bifidobacteria and lactobacilli isolated from dogs and primates. Anaerobe. 2014;29:108–12.
28. Dulay SB, Gransee R, Julich S, Tomaso H, O' Sullivan CK. Automated microfluidically controlled electrochemical biosensor for the rapid and highly sensitive detection of *Francisella tularensis*. Biosens Bioelectr. 2014;59:342–9.
29. Eisenberg D. Surgical site infections: time to modify the wound classification system? J Surg Res. 2012;175:54–5.
30. Ortega G, Rhee DS, Papandria DJ, et al. An evaluation of surgical site infections by wound classification system using the ACS-NSQIP. J Surg Res. 2012;174:33–8.
31. Klodzinska E, Kupczyk W, Jackowski M, Buszewski B. Capillary electrophoresis in the diagnosis of surgical site infections. Electrophoresis. 2013;34:3206–13.
32. Fon Sing S, Isdepsky A, Borowitzka MA, Lewis DM. Pilot-scale continuous recycling of growth medium for the mass culture of a halotolerant *Tetraselmis* sp. in raceway ponds under increasing salinity: a novel protocol for commercial microalgal biomass production. Bioresour Technol. 2014;161:47–54.
33. Goetz K, Pass T, Wright R, Collins K. Potential new method: a comparability study of M-coliblue24 and M-endo les agar for the verified recoveries of total coliforms and *E. coli*. Abst Gen Meeting Am Soc Microbiol. 1997;97:481.
34. Balazova T, Makovcova J, Sedo O, Slany M, Faldyna M, Zdrahal Z. The influence of culture conditions on the identification of *Mycobacterium* species by MALDI-TOF MS profiling. FEMS Microbiol Lett. 2014;353:77–84.
35. Lim KT, Hanifah YA, Yusof MYM, Thong KL. Investigation of toxin genes among methicillin-resistant *Staphylococcus aureus* strains isolated from a tertiary hospital in Malaysia. Trop Biomed. 2012;29:212–9.
36. Sauer S, Freiwald A, Maier T, et al. Classification and identification of bacteria by mass spectrometry and computational analysis. PLoS ONE. 2008;3:1–10.
37. Stomeo F, Valverde A, Pointing SB, et al. Hypolithic and soil microbial community assembly along an aridity gradient in the Namib Desert. Extremophiles. 2013;17:329–37.
38. Smerkova K, Dostalova S, Skutkova H, et al. Isolation of Xis Gen fragment of lambda phage from agarose gel using magnetic particles for subsequent enzymatic DNA sequencing. Chromatographia. 2013;76:329–34.
39. Nagy E. Matrix-assisted laser desorption/ionization time-of-flight mass spectrometry: a new possibility for the identification and typing of anaerobic bacteria. Future Microbiol. 2014;9:217–33.
40. Kuczynski J, Lauber CL, Walters WA, et al. Experimental and analytical tools for studying the human microbiome. Nat Rev Genet. 2012;13:47–58.
41. Somashekar BS, Amin AG, Tripathi P, et al. Metabolomic signatures in guinea pigs infected with epidemic-associated W-Beijing strains of *Mycobacterium tuberculosis*. J Proteome Res. 2012;11:4873–84.
42. Liu W, Zou DY, Wang XS, et al. Proteomic analysis of clinical isolate of *Stenotrophomonas maltophilia* with bla(NDM-1), bla(L1) and bla(L2) beta-lactamase genes under imipenem treatment. J Proteome Res. 2012;11:4024–33.
43. Pereira F, Carneiro J, Matthiesen R, et al. Identification of species by multiplex analysis of variable-length sequences. Nucleic Acids Res. 2010;38:1–17.
44. Kolbert CP, Persing DH. Ribosomal DNA sequencing as a tool for identification of bacterial pathogens. Curr Opin Microbiol. 1999;2:299–305.
45. Zacharioudakis IM, Zervou FN, Ziakas PD, Mylonakis E. Meta-analysis of methicillin-resistant *Staphylococcus aureus* colonization and risk of infection in dialysis patients. J Am Soc Nephrol. 2014;25:2131–41.
46. Ahmed EF, Gad GFM, Abdalla AM, Hasaneen AM, Abdelwahab SF. Prevalence of methicillin resistant *Staphylococcus aureus* among Egyptian patients after surgical interventions. Surg Infect. 2014;15:404–11.

47. Clarke SR, Foster SJ. Surface adhesins of *Staphylococcus aureus*. In: Poole RK, editor. Advances in microbial physiology, vol 51. London: Academic Press Ltd./Elsevier Science Ltd.; 2006. p. 187–225.
48. Rettinger A, Krupka I, Grunwald K, et al. *Leptospira* spp. strain identification by MALDI TOF MS is an equivalent tool to 16S rRNA gene sequencing and multi locus sequence typing (MLST). BMC Microbiol. 2012;12:1–14.
49. Karger A, Stock R, Ziller M, et al. Rapid identification of *Burkholderia mallei* and *Burkholderia pseudomallei* by intact cell matrix-assisted laser desorption/ionisation mass spectrometric typing. BMC Microbiol. 2012;12:1–15.